Shogo Nishikawa, Taishi Kobayashi*, Takayuki Sasaki and Ikuji Takagi

Solubilities and solubility products of thorium hydroxide under moderate temperature conditions

https://doi.org/10.1515/ract-2017-2917
Received December 15, 2017; accepted February 7, 2018; published online March 30, 2018

Abstract: The Th solubilities of the sample solutions that initially contained $Th(OH)_4$(am) prepared by undersaturation and oversaturation methods in the pH_c range of 2.0–8.0 in a 0.5 M ionic strength solution of $NaClO_4$ and $HClO_4$ and stored at aging temperatures (T_a) of 298, 313 and 333 K were investigated in this study. After a certain period of time up to 40 weeks depending on T_a, supernatants of the sample solutions were ultrafiltrated through 3 kDa membranes under the measurement temperature (T_m) of 298, 313 and 333 K. Size distributions of the colloidal species were investigated by ultrafiltration using membranes with different pore sizes ranging from 3 to 100 kDa, and the solid phases were examined by X-ray diffraction (XRD). The solubility of the sample solutions obtained after aging at $T_a = 298$ K using undersaturation method with continuous shaking was similar to those of dried precipitate of Th hydroxide. The solubilities obtained after aging at $T_a = 313$ and 333 K were lower than those at $T_a = 298$ K. The XRD spectra suggested that the crystallization of the solid phase proceeded under these elevated temperatures. The solubility of the sample solutions obtained after aging at $T_a = 333$ K using the oversaturation technique were similar to those prepared by undersaturation method and aged at the same T_a. A slight temperature dependence of the apparent solubilities on the T_m was observed in the sample solutions prepared by both methods. The solubility products ($K_{sp,T_a}(T_m)$) after different T_a and T_m were determined from the solubility analysis. The observed increase in the formation constant ($K_{s,T_a}(T_m)$) of $Th^{4+} + (4+x)H_2O(l) \rightleftharpoons Th(OH)_4 \cdot xH_2O(s,T_a) + 4H^+$ with increasing T_m indicated that the reaction was endothermic. The enthalpy change ($\Delta_r H^\circ_{m_T_a \rightarrow cr}$) between the solid phases of $Th(OH)_4 \cdot xH_2O(s,T_a)$ and ThO_2(cr) suggested that the solid phase transformation from $Th(OH)_4 \cdot xH_2O(s,T_a)$ to ThO_2(cr) contains an endothermic process.

***Corresponding author: Taishi Kobayashi,** Department of Nuclear Engineering, Kyoto University, Kyoto, Japan,
E-mail: kobayashi@nucleng.kyoto-u.ac.jp
Shogo Nishikawa, Takayuki Sasaki and Ikuji Takagi: Department of Nuclear Engineering, Kyoto University, Kyoto, Japan

Keywords: Thorium, hydroxide, oxide, solubility, solubility product, solid phase, temperature effect.

1 Introduction

The safety assessment for the disposal of radioactive waste requires understanding the migration behavior of radionuclides in the near and far fields of repository sites. The migration behavior of tetravalent actinides (An(IV)) is primarily controlled by the sparingly soluble solid phase. Amorphous hydroxides ($An(OH)_4$(am)) are considered as the dominant solubility-limiting solid phases under relevant geochemical conditions [1–4]. Therefore, An(IV) solubility can be described by the solubility products (K_{sp}) of $An(OH)_4$(am) and the complex formation constants ($\beta_{m,n}$) with complexing ligands present in underground water. Extensive studies have been dedicated to determining these thermodynamic constants, and critical reviews of the data used in the relevant literature were performed to establish reliable databases under standard conditions of 298 K and 1 atm [5–7].

Meanwhile, decay heat of the radioactive waste is transferred to groundwater aquifers through surrounding engineered and geological barrier systems in the repositories. The actual temperature evolution in a repository depends on the heat production of radioactive waste and on the disposal concept. For instance, the maximum temperature inside and outside the buffer material for the high-level wastes in the Japanese hard rock repository system were estimated to be 373 K and 353 K, respectively [8]. Simulations of the temperature evolution also suggested that the temperature outside the buffer material in the hard rock system after a thousand years would approximately be 333 K [8]. On the other hand, a much higher temperature, up to 473 K, was estimated for rock salt formation [9, 10]. This indicates the possible migration of radionuclides through the repository systems under elevated temperature conditions above 298 K, especially under early waste package failure scenarios. The impact of elevated temperatures on the An(IV) solubility limits must be clarified for reliable safety assessment of the radioactive waste disposal.

To establish a thermodynamic description of An(IV) solubility under elevated temperatures, it is necessary to consider both the solid phase transformation of $An(OH)_4(am)$ by temperature and the temperature dependence of thermodynamic constant (K_{sp}, $\beta_{m,n}$). With regard to the transformation of solid phase, it is well known that solid $An(OH)_4(am)$ without any X-ray diffraction (XRD) signature can be converted into the thermodynamically stable solid phase well defined as crystalline oxide $AnO_2(cr)$ by heating or calcination at least several hundred degrees [11, 12]. The dehydration and crystallization of $An(OH)_4(am)$ to $AnO_2(cr)$, accompanied by a significant decrease in apparent solubility, was also observed in an aqueous system at elevated temperatures, but well below the crystallization temperature in non-aqueous system. Considering thorium (Th), which exists in a stable tetravalent oxidation state in aqueous systems, amorphous hydroxide of $Th(OH)_4(am)$ is an initial solubility-limiting solid phase that can be converted to the solid phase with less solubility after aging at 363 K [13, 14]. The solubility values were about three orders of magnitude lower than those of $Th(OH)_4(am)$, and the XRD spectra of the solid phases showed several peaks corresponding to those of $ThO_2(cr)$ [13, 14]. The solubility values after aging at 363 K were still a few orders of magnitude higher than those of $ThO_2(cr)$, and the particle size of the solid phase determined by the XRD spectra was rather small compared to that of $ThO_2(cr)$ [14]. Therefore, the solid phase was defined as a unique $Th(OH)_4(s)$ that likely formed by the partial dehydration and crystallization of $Th(OH)_4(am)$ [14]. The observed trend of the K_{sp} values as a function of particle size was discussed and explained based on the suggested particle size effect. It was found that the log K_{sp} value has an inverse proportion with the particle size of the solid phase; thus, the log K_{sp} value decreases as the particle size increases [7].

The temperature dependence of thermodynamic constants such as K_{sp} and $\beta_{m,n}$, is another significant factor to predict the An(IV) solubility at elevated temperatures. Among the critical literature reviews of the Th thermodynamic data performed by the Nuclear Energy Agency Thermochemical Database (NEA-TDB) project [7], only Baes et al. and Ekberg et al. reported the values of hydrolysis constants at temperatures lower or higher than 298 K [15, 16]. For example, Baes et al. studied the hydrolysis of Th at 273 and 368 K in 1 mol/dm^3 (M) $NaClO_4$ using potentiometric titration technique. The temperature dependences of $\beta_{m,n}$ for $ThOH^{3+}$, $Th(OH)_2^{2+}$, $Th_2(OH)_2^{6+}$, $Th_4(OH)_8^{8+}$ and $Th_6(OH)_{15}^{9+}$ were investigated to determine the enthalpy and entropy of the reactions [15]. Ekberg et al. combined the potentiometric titration and solvent extraction techniques, and determined the hydrolysis constants of $ThOH^{3+}$, $Th(OH)_2^{2+}$, $Th(OH)_3^{+}$, $Th(OH)_4(aq)$, $Th_4(OH)_8^{8+}$ and $Th_6(OH)_{15}^{9+}$ at 288, 298 and 308 K [16]. Considering these studies, the recommended enthalpy and entropy for the reactions of $ThOH^{3+}$, $Th(OH)_2^{2+}$, $Th_2(OH)_2^{6+}$, $Th_4(OH)_8^{8+}$ and $Th_6(OH)_{15}^{9+}$ were selected for the literature review [7]. A recent study by Teksöz et al. also examined the hydrolytic behavior of Th at various temperatures of up to 318 K using potentiometric titration technique [17]. The study determined the hydrolysis constants and the enthalpy and entropy for the reactions of the same species as those reported by Ekberg et al. Despite the uncertainties and discrepancies between these reported values as well as lacking data, the hydrolysis constants at elevated temperatures can be estimated based on the values in the literature. On the other hand, very limited data have been reported on the temperature dependence of K_{sp} for $Th(OH)_4(am)$ and/or $Th(OH)_4(s)$ because the chemical conditions of $Th(OH)_4(am)/Th(OH)_4(s)$ are subject to temperature as discussed above. Only Rai et al. measured the solubility of $ThO_2(am{\rightarrow}c)$ and determined its K_{sp} value at 363 K [13]. In the previous study, the solubility of zirconium hydroxides, which is a chemical analog of An(IV), was measured at various aging temperatures (T_a) and measurement temperatures (T_m) to distinguish the effect of solid phase transformation by temperature and temperature dependence of K_{sp} [18]. The apparent solubility was observed to be almost independent of T_m, and the temperature dependence of K_{sp}, $\beta_{m,n}$, and ion product of water (K_w) was considered to be eliminated within the investigated temperature range [18].

The focus of the present study is on the moderate temperature conditions, which are likely to be reached a long time after disposal. In order to determine the K_{sp} values as a function of T_m, sample solutions of $Th(OH)_4(am)$ were first aged at $T_a = 298$, 313 and 333 K and then cooled to different T_m ranging from 298 to 333 K. As in previous studies [14, 18, 19], unique solid phases expressed as $Th(OH)_4 \cdot xH_2O(s, T_a)$ after aging at respective T_a were defined. Based on the dependence of formation constant (K_s) for $Th^{4+} + (4+x)H_2O(1) \rightleftharpoons Th(OH)_4 \cdot xH_2O(s, T_a) + 4H^+$ on T_m, the enthalpy of the reaction ($\Delta_r H^\circ$) was calculated for each solid phase. The observed trend in the $\Delta_r H^\circ$ values was analyzed to understand the solid-phase transformation of $Th(OH)_4(am)$ at elevated temperatures. The impact of elevated temperatures on the apparent Th solubility was discussed considering the solid phase transformation and temperature dependence of K_s and $\beta_{m,n}$.

2 Experimental methods and materials

2.1 Chemicals and analytical methods

All chemicals used in the experiments were reagent grade. $Th(NO_3)\cdot 4H_2O$ were purchased from Nakalai Chemicals Ltd. and $HClO_4$, NaOH, $NaClO_4$ and NaCl were purchased from Wako Pure Chem. All solutions were prepared with deionized purified water (Milli-Q, Millipore). $Th(NO_3)\cdot 4H_2O$ was dissolved into purified water and portions of NaOH solution were then added to the thorium nitrate solution to neutralize and precipitate thorium hydroxide ($Th(OH)_4$(am)). The precipitate was washed with purified water and finally suspended in purified water as a $Th(OH)_4$(am) stock suspension for the solubility experiment by undersaturation method. To perform a solubility experiment using the oversaturation technique, a portion of $Th(OH)_4$(am) was dissolved in 0.1 M $HClO_4$ to obtain the Th aqueous solution ([Th] = 0.3 M). A combination glass electrode (9615-10D, Horiba Ltd.) was used to measure the hydrogen ion concentrations (pH_c). The internal solution of the electrode consisted of 3.6 M NaCl and 0.4 M $NaClO_4$ to prevent the precipitation of $KClO_4$ at the junction of the electrode and the solution. The electrode was calibrated against standard HCl solutions (Wako Pure Chem.) at T_m = 298, 313 and 333 K and at ionic strength (I) = 0.5 M to correct the experimentally measured pH_{exp} values corresponding to their calculated pH_c values at the respective temperatures.

2.2 Solubility experiments

Sample solutions were prepared in an Ar glove box (O_2 <1 ppm) at 298 K using both oversaturation and undersaturation methods. For the undersaturation method, an aliquot of $NaClO_4$, $HClO_4$ and/or NaOH solutions were added into polypropylene tubes to prepare sample solutions of a specific pH_c and ionic strength (I). The initial pH_c ranged from 2.0 to 8.0 and the ionic strength was fixed at I = 0.5 M. A small amount of $Th(OH)_4$(am) stock suspension was then added to the polypropylene tubes such that the Th concentration corresponded to 0.01 M if the solid phase was completely dissolved. For the oversaturation method, a 100 mL of initial Th perchlorate ([Th] = 0.01 M) was obtained from the Th stock solution ([Th] = 0.3 M). The pH condition was adjusted to the desired pH within the range from 2.0 to 8.0 by adding $HClO_4$ and/or NaOH to the initial Th solution using a magnetic stirrer to stir the solution. A 10 mL of aliquots was withdrawn and collected in polypropylene tubes at each desired pH value. The ionic strength was fixed at I = 0.5 M by adding the appropriate amounts of $NaClO_4$.

The sample tubes prepared by the undersaturation method were placed and stored in a constant temperature shaking incubator (BR-43FL MR, Titec). The aging temperature (T_a) conditions were T_a = 298, 313 and 333 K and the shaking speed was set at 70 rpm. After given periods, the sample solutions were removed from the shaking incubator and placed in thermostated baths maintained at a measurement temperature (T_m) corresponding to each T_a. The pH measurements and ultrafiltration of the sample solutions at T_m (=T_a) were then performed. A desktop centrifuge (FB-4000, Kurabo) introduced in a temperature chamber was used to filtrate the sample solutions at T_m = 298, 313 and 333 K. The observed pH values at different temperatures were corrected to their pH_c values using temperature-specific calibration curves that were determined by Kobayashi et al. [18]. The supernatant of the sample solutions was filtrated using ultrafiltration membranes-based device (Microcon NMWL 3–100 kDa, corresponding to approximately 2–7 nm pore sizes, Millipore). After the pH measurement and ultrafiltration at each T_m, the sample solutions were returned to the environmental test chambers with controlled temperatures set at T_a = 298, 313 and 333 K. The solubility measurement at $T_m = T_a$ = 298, 313 and 333 K was repeated for several months until the steady state was confirmed. Then, the sample solutions after aging at T_a were cooled down to T_m ($T_m < T_a$) using the thermostat baths and kept for 1 day prior to the pH measurement and ultrafiltration at T_m. The sample tubes prepared by the oversaturation technique were placed and stored in an environmental test chamber (EOP-450B, Asone) with controlled temperature set at T_a = 333 K for predetermined aging periods of up to 30 weeks. The sample tubes were sometimes manually shaken for few minutes during the aging process. After given periods, the sample tubes were taken from the test chamber and cooled down and maintained at T_m = 298 K for 1 day. The pH_c of the sample solutions was measured and the supernatants were filtrated through 3 kDa membranes at T_m = 298 K. After the pH measurement and ultrafiltration were performed, the sample solutions were returned to the test chamber and the solubility measurements were repeated until the steady state was achieved. The sample solutions after aging at T_a = 333 K were then measured at T_m = 298, 313 and 333 K in the same manner as that in the undersaturation experiment after being kept at each T_m for 1 day. The sample conditions are summarized in Table 1.

Table 1: Summary of samples under given aging and measurement temperature conditions.

Preparation method	Aging temperature T_a[b] (K)	Measurement temperature T_m[a] (K)		
		298	313	333
Undersaturation	298	(am)[c]→(s,298)[d]	–	–
	313	(am)[c]→(s,313)[d]	(am)[c]→(s,313)[d]	–
	333	(am)[c]→(s,333)[d]	(am)[c]→(s,333)[d]	(am)[c]→(s,333)[d]
Oversaturation	333	(am)[c]→(s,333)[d]	(am)[c]→(s,333)[d]	(am)[c]→(s,333)[d]

[a]Temperature during the pH measurement and ultrafiltration.
[b]Temperature during aging in the environmental test chamber.
[c]Freshly precipitated amorphous $Th(OH)_4$ at 298 K.
[d]Solid phases formed after aging the sample solutions at 298, 313, or 333 K.

After ultrafiltration, a small amount of nitric acid was added in the filtrate immediately to avoid sorption of Th species on the sample tube throughout the solubility experiment. The filtrate was diluted in 0.01 M nitric acid and then measured by inductively coupled plasma mass spectrometry (ICP-MS) (HP4500, Hewlett Packard) to determine the Th concentration. The detection limit of Th was approximately 10^{-8} M. The standard error was within 10 % for each measurement by ICP-MS, which resulted in ±0.1 in the log unit of Th concentration.

2.3 Solid-phase analysis

After the solubility experiment, the solid phases were separated by centrifugation from several sample solutions and dried at 298 K and atmospheric pressure. The solid phases were then investigated by XRD methods (RINT2000, Rigaku) using a Cu X-ray ($\lambda_{K\alpha}$ = 1.54 Å) within the range of $2\theta = 20° - 60°$. For comparison, the XRD patterns were also obtained for commercial ThO_2 powder (Nakalai Chemicals Ltd.) and freshly precipitated $Th(OH)_4$(am) at 298 K.

3 Results and discussion

3.1 Solubilities of $Th(OH)_4 \cdot xH_2O(s, T_a)$ aged and measured at 298–333 K by undersaturation method

3.1.1 Effects of aging temperature at 298–333 K

Figure 1 shows the solubility of Th hydroxide aged at 298 K with continuous shaking. The solubility was measured at 298 K after ultrafiltration through 3 kDa membranes. The data collected from relevant literature on the solubility of Th hydroxide prepared by undersaturation approach is also presented [13, 20–22]. As similar solubility values were obtained after 62 and 81 days, the steady state was considered to be achieved within 2 months. Similar or shorter equilibrium time has been pointed out in the literature [13, 21, 22]. No systematic dependence of the solubility on the pore size of ranging from up 3 to 100 kDa was observed, suggesting a limited contribution of colloidal species to the apparent solubility, in contrast to the case when the sample solutions were prepared by oversaturation method [24]. It is noted that the obtained solubility values in this study were similar to the literature data, where the solubility experiment started from dried precipitate of Th hydroxide [21, 22]. Östhols et al. prepared an aqueous Th nitrate solution and quickly added NaOH to precipitate Th hydroxide. After washing the precipitate with water, it was dried at room temperature for 1 week in a vacuum desiccator [21]. Neck et al. followed a similar approach to prepare the solid phase as that adopted by Östhols et al. They indicated that the dried solid phase consisted of a "non-unique hydrated oxyhydroxide $ThO_n(OH)_{4-2n} \cdot xH_2O$(am)" with a hydroxide surface layer [22]. As these studies also confirmed that there is a limited effect of colloidal species on the apparent solubility [21, 22], the similarity in the apparent solubility values between the present investigation and these studies was attributed to the similarity in the solubility-limiting solid phase. Extra dehydrated solid phase might be obtained in this study after continuous shaking at 298 K.

Lower Th solubility values were obtained after aging at T_a = 313 K with continuous shaking than those measured at T_a = 298 K, and the steady state was reached within a few weeks. The solubility values aged at T_a = 313 K for 236 and 280 days and measured at T_m = 298 K after ultrafiltration through 3 kDa membranes were plotted, and are shown in Figure 1. The observed values were approximately one or two orders of magnitude lower than those obtained at T_a = 298 K. Th solubility values obtained after aging at T_a = 333 K and measured at T_m = 298 K show

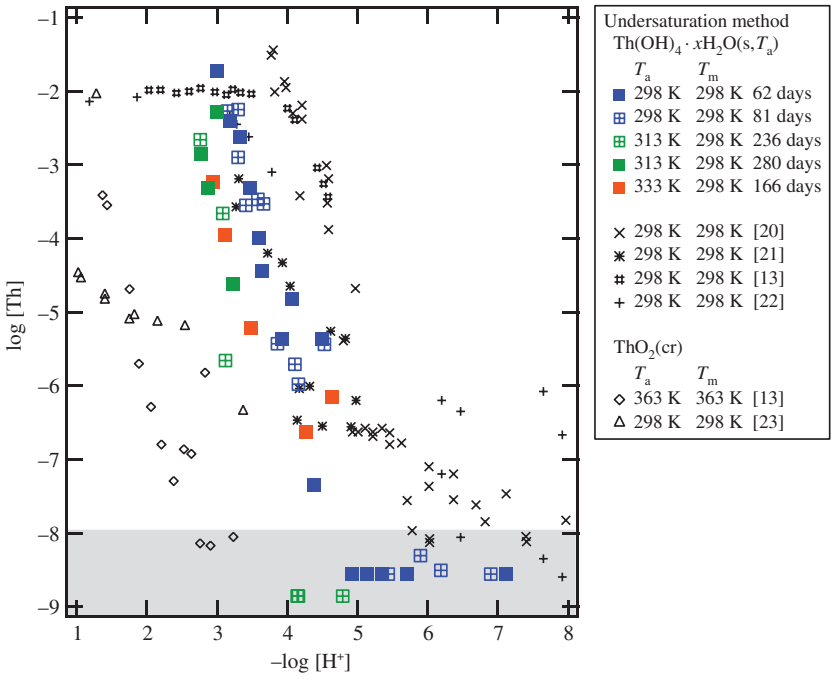


Figure 1: Solubilities of $Th(OH)_4 \cdot xH_2O(s,T_a)$ (3 kDa ultrafiltration, $I = 0.5$) after aging at $T_a = 298–333$ K and measured at $T_m = 298$ K. The sample solutions were prepared by undersaturation method. The gray field represents the detection limit of ICP-MS.

similar values to those obtained at $T_a = 313$ K. In addition, the solubility of ThO_2(cr) aged and measured at the respective temperatures of 298 and 363 K [13, 23] is presented in Figure 1 for comparison. The solubility data of ThO_2(cr) were still more than a few orders of magnitude lower than those of $Th(OH)_4 \cdot xH_2O(s,T_a)$ defined as the solid phase aged at T_a ($T_a = 313$ and 333 K). Since the solubility of $Th(OH)_4 \cdot xH_2O(s,T_a)$ after aging at $T_a = 313$ and 333 K

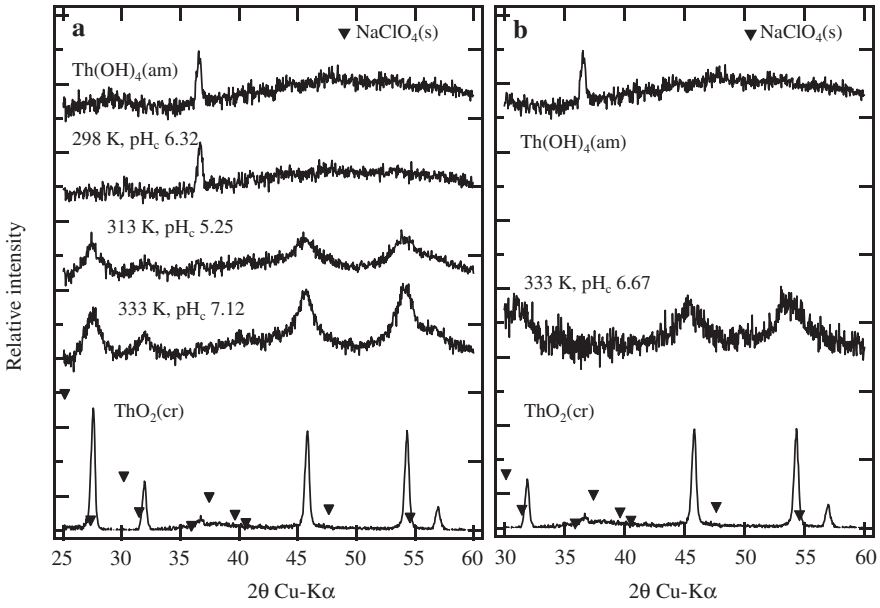


Figure 2: XRD patterns of Th solid phases (a) prepared by undersaturation method and aged at $T_a = 298$, 313 and 333 K ($I = 0.5$) (b) prepared by oversaturation method and aged at $T_a = 333$ K ($I = 0.5$), compared to ThO_2(cr), freshly precipitated $Th(OH)_4$(am) and $NaClO_4$(s) as references.

showed a clear pH dependence up to near the Th concentration of total dissolution of the solid phases, it was obviously suggested that the solubility was not controlled by fully crystalline ThO_2(cr) but another solid phase obtained under the elevated temperature conditions. Comparing the solubility with those aged at 298, 313 and 333 K, further solid phase transformation was considered to occur at 313 K.

Figure 2a shows typical XRD spectra of the Th solid phases aged under the neutral pH_c condition at $T_a = 298$, 313 and 333 K, together with those of ThO_2(cr) and freshly precipitated $Th(OH)_4$(am). No significant peak was observed in the XRD spectra of the solid phase aged at 298 K, indicating that the solid phase has no crystalline bulk structure as well as that of freshly precipitated $Th(OH)_4$(am). A sharp peak was observed at 36.4°, corresponding to that of $NaClO_4$ (JCPDS 80494) at 37.4°, which was used to adjust the ionic strength that might contaminate the sample during the separation process of the solid phase. Minor peaks of $NaClO_4$ were not shown possibly due to the limited amount and inhomogeneous deposition of $NaClO_4$ during the drying process of the samples. Although the apparent solubility of $Th(OH)_4 \cdot xH_2O(s, T_a)$ aged at $T_a = 298$ K with continuous shaking was lower than those of $Th(OH)_4$(am), the XRD spectra suggested that the crystallization did not proceed at 298 K. In contrast, broad peaks at 27.6°, 32.0°, 45.9° and 54.4° corresponding to those of ThO_2(cr) were observed after aging at $T_a = 313$ and 333 K. This indicates the existence of crystalline structure in the solid phase. The width of the peak in the XRD pattern is inversely proportional to the crystalline particle size of the solid phase. Based on the Scherrer equation [25], the particle size (D) is given as

$$D = K\lambda / (\beta - B)\cos\theta \quad (1)$$

where K, λ (nm), β, B and θ (°) represent the Scherrer constant (0.94), X-ray wavelength (0.154 nm for Cu-Kα), the line full width at half maximum intensity (FWHM) of the peak in radians, the background broadening and the Bragg angle, respectively. The background broadening, B, was set at 0.19° by measuring a large single crystal of Al_2O_3.

Equation (1) was used to calculate the crystalline size of the Th solid phase particles after aging at 313 and 333 K for the peaks observed at 27.6°, 45.9° and 54.4°, as listed in Table 2. The peak at 32.0° was not considered in the present analysis owing to the low intensity. The crystalline size of the solid phases, determined following the Scherrer equation, was approximately 4–6 nm, and no significant difference depending on the pH_c and the aging temperature of 313 and 333 K was confirmed. The similarity between the solubility data obtained after aging at 313 and 333 K shown in Figure 1 reflects the similar solid phase crystalline sizes.

3.1.2 Effects of measurement temperatures at 278–333 K

After aging the sample solutions at $T_a = 313$ and 333 K, the solubilities were investigated at different measurement temperatures of $T_m = 298$, 313 and 333 K. To avoid further transformation of the solid phase during the solubility measurement, T_m was kept lower than T_a. Figure 3a shows the Th solubility obtained after aging at 313 K and measured at 298 and 313 K, while Figure 3b displays the Th solubility after aging at 333 K and measured at 298, 313 and 333 K. Considerably small differences between the solubility data at different T_m values were observed in both cases. The limited impact of T_m on the apparent solubility was also observed in the solubility of Zr hydroxide solid phases after aging at 298, 313 and 333 K [18].

Table 2: Crystalline size of Th solid phase particles after aging at $T_a = 298–333$ K.

Preparation method	Aging temperature T_a (K)	pH_c	Crystalline size (nm)[a]		
			Peak position		
			27.6°	45.9°	54.4°
Undersaturation	298	6.32	–	–	–
	313	5.25	5.7 ± 0.2	4.6 ± 0.2	3.2 ± 0.1
	313	9.37	5.9 ± 0.4	4.1 ± 0.3	4.1 ± 0.2
	333	5.41	6.5 ± 0.1	6.0 ± 0.3	3.5 ± 0.1
	333	7.12	5.9 ± 0.3	6.0 ± 0.2	4.1 ± 0.1
Oversaturation	333	6.67	–	3.7 ± 0.2	3.3 ± 0.1

[a]The error indicates the standard error.

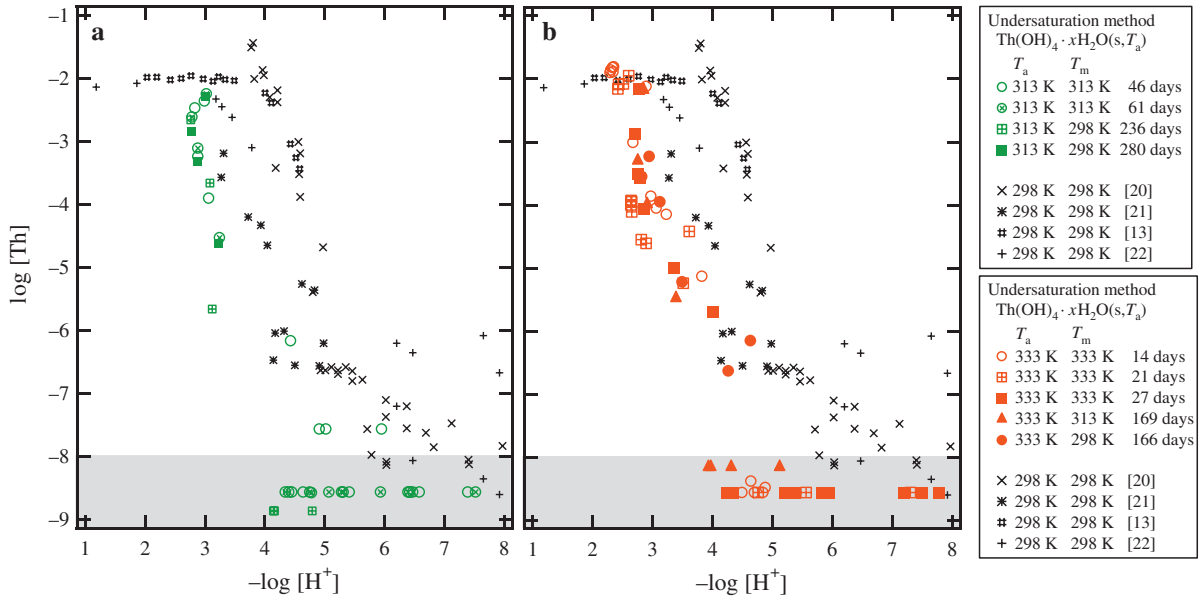


Figure 3: Solubilities of $Th(OH)_4 \cdot xH_2O(s,T_a)$ (3 kDa ultrafiltration, $I = 0.5$); (a) after aging at $T_a = 313$ K and measured at $T_m = 298$ and 313 K. (b) after aging at $T_a = 333$ K and measured at $T_m = 298$, 313 and 333 K. The sample solutions were prepared by undersaturation method. The gray field represents the detection limit of ICP-MS.

3.2 Solubilities of $Th(OH)_4 \cdot xH_2O(s,T_a)$ aged and measured at 298–333 K by oversaturation method

3.2.1 Effects of aging temperature at 333 K

Th solubilities of the sample solutions prepared by oversaturation method, after aging at 333 K and measured at 298 K after ultrafiltration through 3 kDa membranes are shown in Figure 4. The obtained solubility after 62 and 122 days was approximately three orders of magnitude lower than those obtained at $T_a = 298$ K using oversaturation technique within the pH_c range of 3–5 [24]. This indicates the transformation of solubility-limiting solid phase. Th solubility of the sample solution prepared by undersaturation method, after aging at 333 K and measured at 298 K previously shown in Figure 1 was also plotted in Figure 4 for comparison. The oversaturation technique involved occasional manual shaking of the sample solutions for a few minutes, while those prepared by undersaturation method were continuously shaken. As shown in Figure 4, the obtained Th solubility values from the oversaturation and undersaturation preparation methods are in good agreement despite the different preparation and aging conditions. This confirms that a steady state was reached in the system when $T_a = 333$ K and $T_m = 298$ K. In contrast different solubilities were more prominent between the sample solutions prepared by oversaturation and undersaturation methods when $T_a = T_m = 298$ K. Aging the sample solutions at elevated temperature might accelerate the solubility reaction to achieve the steady state.

Figure 2b shows the XRD spectra of the solid phase prepared by oversaturation method and aged at 333 K. Broad peaks at 32.0°, 45.9° and 54.4° were observed corresponding to ThO_2(cr). This indicates that the crystallization process proceeded under the temperature condition of 333 K. The solid phase crystalline sizes of 3.7 and 3.3 nm were calculated using the Scherrer equation for the peaks observed at 45.9° and 54.4°, respectively (see Table 2). The crystalline sizes for the peaks at 27.6° and 32.0° were not obtained owing to the 2θ range of the measurement. The solid phase crystalline size achieved by the oversaturation method at $T_a = 333$ K was comparable to those by the undersaturation method at $T_a = 333$ K within their deviation of the crystalline sizes at different peak positions as shown in Table 2.

3.2.2 Effects of measurement temperatures at 278–333 K

Figure 5 shows Th solubilities of the sample solutions prepared by oversaturation method, after aging at $T_a = 333$ K and measured at $T_m = 298$, 313 and 333 K after ultrafiltration through 3 kDa membranes. The solubilities obtained after aging at $T_a = 333$ K were influenced by the

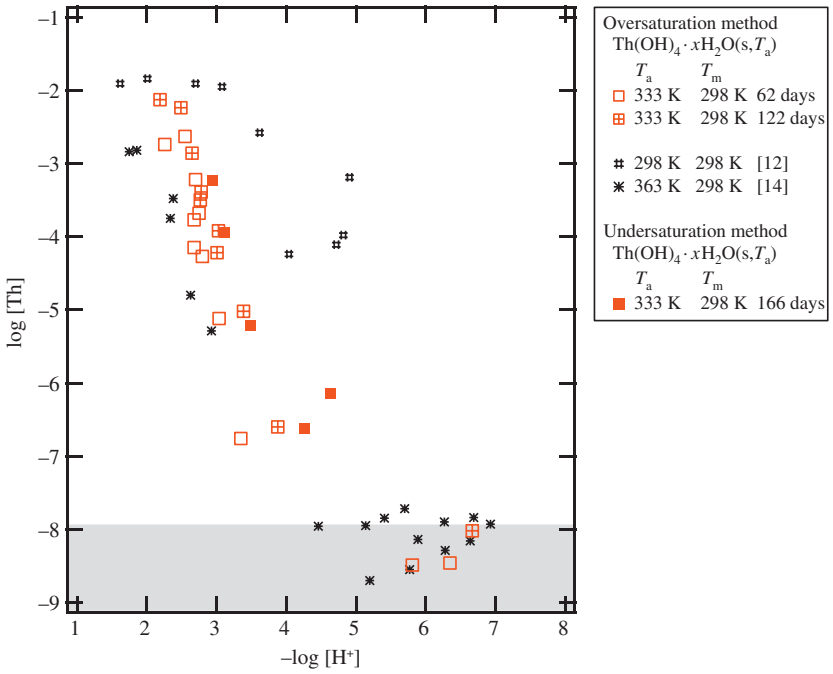


Figure 4: Solubility of $Th(OH)_4 \cdot xH_2O(s,T_a)$ (3 kDa ultrafiltration, $I = 0.5$) prepared by oversaturation method, aged at $T_a = 333$ K, and measured at $T_m = 298$ K compared to those prepared by undersaturation method (3 kDa ultrafiltration, $I = 0.5$). The gray field represents the detection limit of ICP-MS.

measurement temperature T_m. The solubility of several samples was measured after aging at $T_a = 333$ K and ultrafiltration through membranes with different pore sizes of up to 100 kDa. No systematic trend in pore sizes was observed, indicating negligible contribution of colloidal species to the apparent solubility. It was reported that the

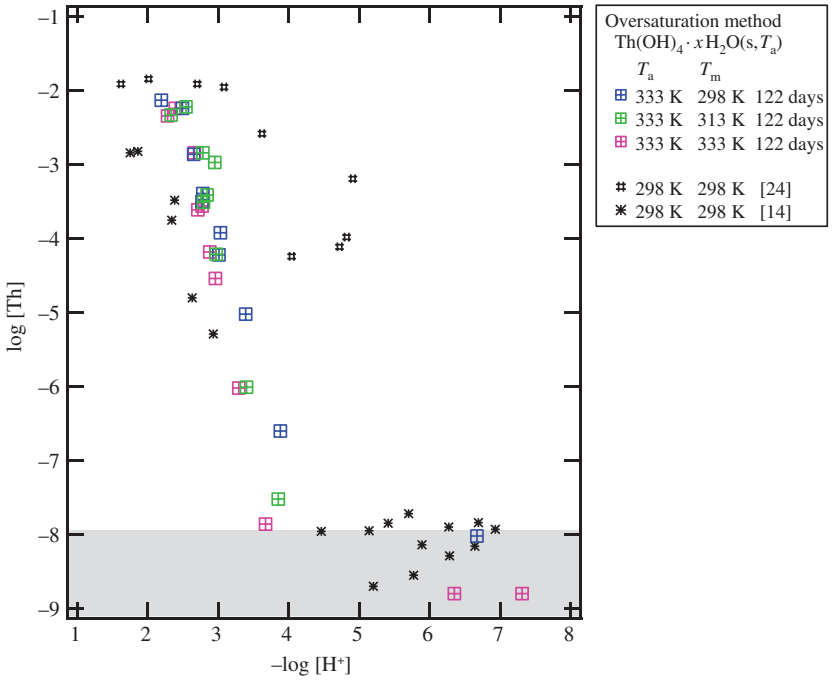


Figure 5: Solubilities of $Th(OH)_4 \cdot xH_2O(s,T_a)$ prepared by oversaturation method, aged at $T_a = 333$ K, and measured at $T_m = 298$, 313 and 333 K (3 kDa ultrafiltration, $I = 0.5$). The gray field represents the detection limit of ICP-MS.

sample solutions prepared by oversaturation method and aged at $T_a = 298$ K contained a colloidal contribution [24] while those aged at $T_a = 363$ K showed negligible impact of the colloidal species [14]. Once the sample solution was heated at elevated temperatures, the colloidal species might be agglomerated and removed from the solution.

3.3 Solubility products of $Th(OH)_4 \cdot xH_2O(s,T_a)$ at $T_a = 278–333$ K

3.3.1 Thermodynamic description of Th solubility at different aging temperatures

As explained in Section 3.1, the apparent solubility of Th hydroxide ($Th(OH)_4 \cdot xH_2O(s,T_a)$) prepared by undersaturation method was found to be independent of the different pore sizes after ultrafiltration through membranes of 3–100 kDa, indicating a limited contribution of colloidal species to the apparent solubility. When the sample solutions were prepared by oversaturation method, formation of stable colloidal species was observed at the aging temperature of 298 K [24]. However, when the sample solution was heated at 363 K, their contribution became negligible [14]. In the present study, no systematic trend in the solubility was observed when different filter pore sizes were used after aging at 333 K; thus, the colloidal species were considered to be removed from the solution by heating at 333 K.

It is widely known that tetravalent actinides (An(IV)) often form not only mononuclear but also polynuclear hydrolysis species and their speciation significantly depends on the total concentration of An(IV). Based on the experimental and estimated hydrolysis constants for mononuclear and polynuclear species, contributions of hydrolysis species were simulated in our previous study [3]. In the case of Th, due to the weaker hydrolysis reaction compared to other actinides, the contribution of polynuclear species were rather limited under the total Th concentration less than 10^{-2} M [3]. In the present study, therefore, mononuclear hydrolysis species were assumed to be dominant soluble species. This is similar to the analysis performed for the solubility data aged at 363 K [14]. The apparent solubility ($[Th]_{tot}$) in the solubility analysis is then described as follows:

$$\begin{aligned}[Th]_{tot} &= [Th^{4+}] + [ThOH^{3+}] + [Th(OH)_2^{2+}] + [Th(OH)_3^{+}] \\ &\quad + [Th(OH)_4(aq)] \\ &= [Th^{4+}]\left(1 + \beta_{1,1}[OH^-] + \beta_{1,2}[OH^-]^2 + \beta_{1,3}[OH^-]^3 + \beta_{1,4}[OH^-]^4\right) \\ &= \frac{K_{sp,T_a}}{[OH^-]^4}\left(1 + \beta_{1,1}[OH^-] + \beta_{1,2}[OH^-]^2 + \beta_{1,3}[OH^-]^3 + \beta_{1,4}[OH^-]^4\right) \end{aligned} \quad (2)$$

where $\beta_{1,n}$ ($n = 1–4$) and K_{sp,T_a} represent the conditional hydrolysis constant and the conditional solubility product of the Th hydroxide ($Th(OH)_4 \cdot xH_2O(s,T_a)$) formed at respective aging temperatures (T_a). The solubility-limiting solid phases were defined depending on the aging temperatures of T_a. The solid phases aged at 298, 313 and 333 K were expressed as $Th(OH)_4 \cdot xH_2O(s,298)$, $Th(OH)_4 \cdot xH_2O(s,313)$ and $Th(OH)_4 \cdot xH_2O(s,333)$, respectively.

3.3.2 Thermodynamic analysis of the solubility data at different aging and measurement temperatures

The thermodynamic analysis of the solubility data aged and measured at different temperatures was described in the previous study on the solubility of Zr hydroxides [18]. In the present study, the solubility product of K_{sp,T_a} for each aging temperature ($T_a = 298$, 313 and 333 K) was also introduced. In order to treat the constant as a function of measurement temperature T_m, the formation constants of K_{s,T_a} and ${}^*\beta_{1,n}$ defined by isocoulombic reactions were introduced.

$$Th^{4+} + (4+x)H_2O(l) \rightleftharpoons Th(OH)_4 \cdot xH_2O(s,T_a) + 4H^+ \quad (3)$$

$$Th^{4+} + nH_2O(l) \rightleftharpoons Th(OH)_n^{(4-n)+} + nH^+ \quad (n = 1–4) \quad (4)$$

The K_{s,T_a} and ${}^*\beta_{1,n}$ were expressed by the integrated van't Hoff equation as functions of measurement temperature T_m.

$$\log K_{s,T_a}(T_m) = \log K_{s,T_a}(T_0) + \frac{\Delta_r H^\circ_{m_T_a}}{R \ln 10}\left(\frac{1}{T_0} - \frac{1}{T_m}\right), \quad (5)$$

$$\log {}^*\beta_{1,n}(T_m) = \log {}^*\beta_{1,n}(T_0) + \frac{\Delta_r H^\circ_{m_1,n}}{R \ln 10}\left(\frac{1}{T_0} - \frac{1}{T_m}\right), \quad (6)$$

where R and T_0 are the universal gas constant and 298 K, respectively. The change in the heat capacity of the reaction was assumed to be zero over the investigated temperature range of 298–333 K. The $\Delta_r H^\circ_{m_Ta}$ and $\Delta_r H^\circ_{m_1,n}$ represented the enthalpies for the reactions of Eqs. (3) and (4), respectively.

Only few studies in the relevant literature were dedicated to the hydrolysis reaction of Th under elevated temperature conditions. Baes et al. investigated the hydrolysis of Th in 1 M $NaClO_4$ at 273, 298 and 368 K using potentiometric titration technique [15]. The titration curve was well reproduced by assuming several mononuclear and polynuclear hydrolysis species such as $ThOH^{3+}$, $Th(OH)_2^{2+}$, $Th_2(OH)_2^{6+}$, $Th_4(OH)_8^{8+}$ and $Th_6(OH)_{15}^{9+}$. Ekberg et al.

Table 3: Summary of the thermodynamic constants of Th hydroxides at different T_a and T_m.

Preparation method	Aging temperature T_a[a] (K)	log $K_{s,T_a}(T_m)$		
		Measurement temperature T_m[b] (K)		
		298	313	333
Undersaturation	298	−7.7 ± 0.4[c]	–	–
	313	−6.2 ± 0.3[c]	−5.9 ± 0.4[c]	–
	333	−6.0 ± 0.1[c]	−4.8 ± 0.5[c]	−4.8 ± 0.1[c]
Oversaturation	298	−8.0 ± 0.1[c] [24]		
	333	−5.8 ± 0.3[c]	−4.8 ± 0.1[c]	−4.4 ± 0.1[c]
	363	−4.4 ± 0.5[c] [14]		

[a]Temperature during aging in the test chamber.
[b]Temperature during the pH measurement and ultrafiltration.
[c]Standard errors.

combined the potentiometric titration and solvent extraction techniques and determined the hydrolysis constants of $ThOH^{3+}$, $Th(OH)_2^{2+}$, $Th(OH)_3^{+}$, $Th(OH)_4(aq)$, $Th_4(OH)_8^{8+}$ and $Th_6(OH)_{15}^{9+}$ at 288, 298 and 308 K [16]. These study findings were considered to determine the recommended enthalpy and entropy values selected for the literature review for the reactions of $ThOH^{3+}$, $Th(OH)_2^{2+}$, $Th_2(OH)_2^{6+}$, $Th_4(OH)_8^{8+}$ and $Th_6(OH)_{15}^{9+}$ [7]. Recently, Teksöz et al. has also examined the hydrolytic behavior of Th at various temperatures up to 318 K using potentiometric titration technique and determined the hydrolysis constants and the enthalpy and entropy of the reactions for the same species reported by Ekberg et al. [17]. As discussed in [7] and [4], although $\Delta_r H^\circ_{m_1,n}$ was reported in some scattered reports and the obtained values are still lacking, these values were used in this study to calculate ${}^*\beta_{1,n}(T_m)$ at each T_m. The $\Delta_r H^\circ_{m_1,n}$ values of 44.2 ± 6.3, 85.7 ± 41.4, 86.3 ± 6.8 and 13.0 ± 8.3 kJ/mol for $ThOH^{3+}$, $Th(OH)_2^{2+}$, $Th(OH)_3^{+}$ and $Th(OH)_4(aq)$, respectively were taken from the literatures [7, 17]. Based on Eq. (2), the solubility can be expressed as

$$[Th]_{mono} = [Th^{4+}] + [ThOH^{3+}] + [Th(OH)_2^{2+}] + [Th(OH)_3^{+}] + [Th(OH)_4(aq)] = \frac{[H^+]^4}{K_{s,T_a}(T_m)}\left\{1 + \frac{{}^*\beta_{1,1}(T_m)}{[H^+]} + \frac{{}^*\beta_{1,2}(T_m)}{[H^+]} + \frac{{}^*\beta_{1,3}(T_m)}{[H^+]^3} + \frac{{}^*\beta_{1,4}(T_m)}{[H^+]^4}\right\}, \quad (7)$$

The $K_{s,T_a}(T_m)$ (T_m = 298, 313 and 333 K) values were determined by a least-squares fitting analysis of the solubility data for the mononuclear species at temperatures range from 298 to 333 K (Figures 3 and 5), using Eq. (7). The ${}^*\beta_{1,n}(T_m)$ values recalculated from the ${}^*\beta^\circ_{1,n}(T_{298})$ values [26] were considered as fixed parameters in the analysis.

The values of ${}^*\beta_{1,n}(T_m)$ and $K_{s,T_a}(T_m)$ were corrected to $I = 0$ using specific-ion-interaction (SIT) theory [6]. The temperature dependence of the Debye–Hückel term (D) was obtained from the literature [6]. The ion-interaction coefficients were assumed to be constant versus the temperature, and ε (Th^{4+}, ClO_4^-), ε ($ThOH^{3+}$, ClO_4^-), ε ($Th(OH)_2^{2+}$, ClO_4^-), ε ($Th(OH)_3^+$, ClO_4^-), and ε (Na^+,OH^-) were set at 0.67, 0.45, 0.3, 0.15, and 0.04 kg/mol, respectively [6, 27]. The obtained $K_{sp,T_a}(T_m)$ values are listed in Table 3. The $K_{sp,T_a}(T_m)$ values in the literature [14, 24] was recalculated to $K_{s,T_a}(T_m)$ using the ion product of water $K_w(T_m)$ values taken from the literature [28].

Figure 6 depicts the log $K_{s,T_a}(T_m)$ values in Table 3 plotted against the inverse aging temperature T_a. When the temperature of measurement T_m was constant (T_m = 313

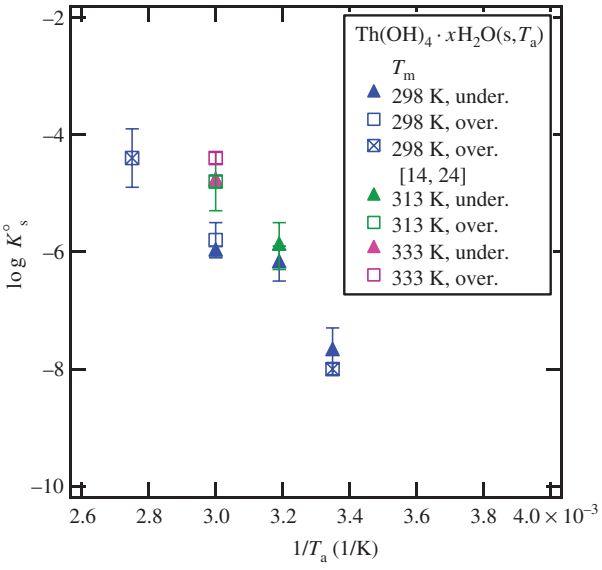


Figure 6: The formation constant of $Th(OH)_4 \cdot xH_2O(s,T_a)$ as a function of the aging temperature.

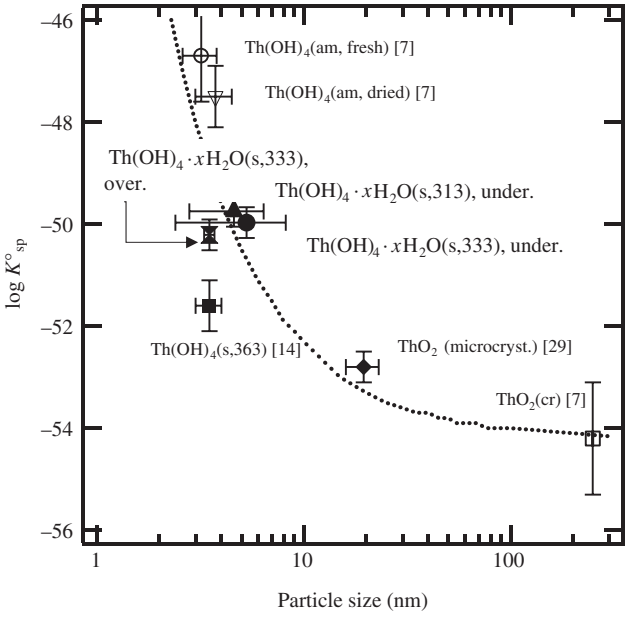


Figure 7: Effect of the particle size on the solubility product of $Th(OH)_4 \cdot xH_2O(s,T_a)$ compared to the different solid phases and predicted curves from the Schindler equation summarized in Ref. [7]. Filled symbols represent the particle sizes experimentally determined in this study and those obtained from the literature, while the open symbols represent the estimated particle sizes.

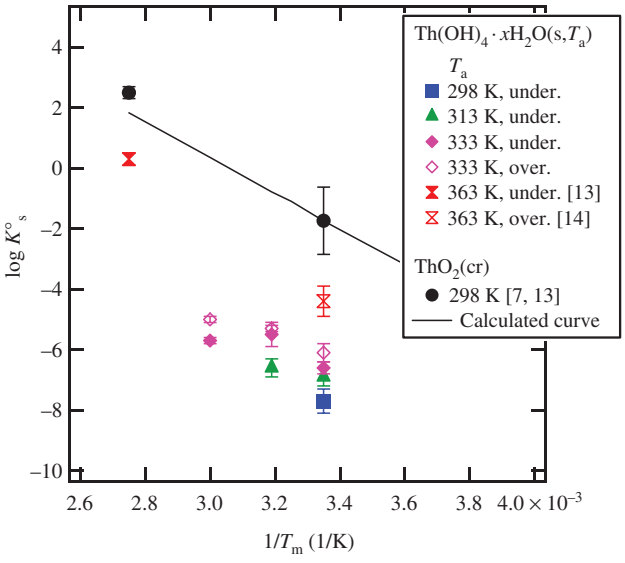


Figure 8: The formation constant of $Th(OH)_4 \cdot xH_2O(s,T_a)$ as a function of the measurement temperature T_m. Solid curve represents the calculated values from the enthalpy and entropy of formation for ThO_2(cr). The plots of $1/T_m = 2.75 \times 10^{-3}$ and 3.35×10^{-3} are from previous studies of samples aged at 298 K and 363 K [7, 13].

and 298 K), $K_{s,T_a}(T_m)$ values increased as T_a increased, indicating the solid phase transformation with less apparent Th solubility. At $T_a = 298$ and 333 K, the plotted log $K_{s,T_a}(T_m)$ from undersaturation and oversaturation methods are comparable to each other.

Figure 7 summarizes the trends of solubility product ($K_{sp,T_a}(T_{298})$) at $T_m = 298$ K for different Th solid phases as a function of particle size [7, 13, 14, 21, 29]. The dotted line represents an estimated solubility product according to the Schindler equation [30]. In the present study, the crystalline size of $Th(OH)_4 \cdot xH_2O$(s,313) and $Th(OH)_4 \cdot xH_2O$(s,333) was determined by analyzing the XRD peaks, and the log $K_{sp,313}(T_{298})$ and log $K_{sp,333}(T_{298})$ are plotted in Figure 7. The error bar in the X-axis for log $K_{sp,313}(T_{298})$ and log $K_{sp,333}(T_{298})$ represents the range of the crystalline sizes at the different peaks and pH_c conditions listed in Table 2. The general trend of log $K_{sp,T_a}(T_m)$ experimental values agreed with the Schindler equation, where $K_{sp,T_a}(T_m)$ decreases as the particle sizes increase. The obtained values of $Th(OH)_4 \cdot xH_2O$(s,313) and $Th(OH)_4 \cdot xH_2O$(s,333) were two or three orders of magnitude lower than those of $Th(OH)_4$(am, fresh) and $Th(OH)_4$(am, dried), and one order of magnitude higher than that of $Th(OH)_4$(s,363) [14]. The log $K_{sp,T_a}(T_m)$ values has the high sensitivity of the particle size obtained in the present analysis deviated depending on the peak in the XRD patterns. The solid phase was considered homogeneous over its bulk and surface in the Schindler equation [7]. To thoroughly understand the particle size effect of the solubility product, further research focusing on the surface properties of the solid phase, which controls the apparent solubility, may be needed.

Figure 8 shows $K_{s,T_a}(T_m)$ values plotted as a function of T_m. Rand et al. [7] reported the enthalpy and entropy of formation for ThO_2(cr) (–1226.4 ± 3.5 kJ/mol and 65.23 ± 0.20 J/K/mol) together with those for Th^{4+}, OH^- and H_2O. The enthalpy and entropy of the reaction of $Th^{4+} + 2H_2O(1) \rightleftharpoons ThO_2(cr) + 4H^+$ were then calculated to be 114.0 ± 6.0 kJ/mol and 348.4 ± 16.7 J/K/mol. The temperature dependence of solubility products of ThO_2(cr) based on the calculated $\Delta_r H^\circ_{m_ThO_2(cr)}$ and $\Delta_r S^\circ_{m_ThO_2(cr)}$ is illustrated by a solid line in Figure 8, together with the values determined in the solubility experiment [13].

$K_{s,T_a}(T_m)$ values of $Th(OH)_4 \cdot xH_2O(s,T_a)$ obtained under different temperature conditions in this study and previous studies are plotted in Figure 8. The $K_{s,T_a}(T_m)$ value for each T_a increased as T_m increased, indicating that $Th^{4+} + (4+x)H_2O(1) \rightleftharpoons Th(OH)_4 \cdot xH_2O(s,T_a) + 4H^+$ reaction was endothermic. The enthalpy ($\Delta_r H^\circ_{m_T_a}$) and entropy ($\Delta_r S^\circ_{m_T_a}$) of the reaction in Eq. (5) could be estimated by a linear-regression analysis of $K_{s,T_a}(T_m)$ values shown in Figure 8. The value of $\Delta_r H^\circ_{m_T_a}$ for the solid phase aged at $T_a = 313$ K was 35.9 ± 59.8 kJ/mol. The values for the solid phase aged at $T_a = 333$ K were 65.5 ± 7.7 and 54.0 ± 12.1 kJ/mol for undersaturation and oversaturation methods, respectively. Although the obtained values are

primarily subject to the values used in the analysis such as $\beta_{1,n}(T_m)$, the enthalpy change $(\Delta_r H^\circ_{m_T_a\to cr})$ between the solid phases of $Th(OH)_4 \cdot xH_2O(s,T_a)$ ($T_a = 313$, 333 K) and ThO_2(cr) suggested that the solid phase transformation from $Th(OH)_4 \cdot xH_2O(s,T_a)$ to ThO_2(cr) contains an endothermic process.

4 Conclusions

Th solubilities of the sample solutions that initially contained $Th(OH)_4$(am) prepared by undersaturation and oversaturation methods were aged at $T_a = 298$, 313 and 333 K and measured at $T_m = 298$, 313 and 333 K. The solubility of the sample solutions obtained after aging at $T_a = 298$ K using undersaturation method with continuous shaking was similar to the solubility of dried precipitate of Th hydroxide. The solubilities of the sample solutions aged at $T_a = 313$ and 333 K were lower than those aged at $T_a = 298$ K and the crystallization of the solid phase was considered to proceed under these elevated temperatures. The solubility values obtained after aging at $T_a = 333$ K using the oversaturation technique were similar to those prepared by undersaturation method and aged at $T_a = 333$ K. A slight temperature dependence of the apparent solubility on the measurement temperature T_m was observed in the sample solutions prepared by both methods. The solubility products obtained after different T_a and T_m were determined from the solubility analysis. The obtained increase in $K_{s,T_a}(T_m)$ values with increasing T_m indicated that $Th^{4+} + (4+x)H_2O(1) \rightleftharpoons Th(OH)_4 \cdot xH_2O(s,T_a) + 4H^+$ reaction was endothermic. On the other hand, the enthalpy change $(\Delta_r H^\circ_{m_T_a\to cr})$ between the solid phases of $Th(OH)_4 \cdot xH_2O(s,T_a)$ and ThO_2(cr) suggested that the solid phase transformation from $Th(OH)_4 \cdot xH_2O(s,T_a)$ to ThO_2(cr) is comprised of an endothermic process.

Acknowledgments: This study was partially conducted under the Visiting Researchers Program of the Kyoto University Research Reactor Institute (KURRI). This work was supported by the JSPS Grant-in-Aid for Young Scientists (B) Grant Number 16K18348.

References

1. Baes, C. F., Mesmer, R. E.: Hydrolysis of Cations, Wiley, New York (1976).
2. Fanghänel, Th., Neck, V.: Aquatic chemistry and solubility phenomena of actinide oxides/hydroxides. Pure Appl. Chem. **74**, 1895 (2002).
3. Moriyama, H., Sasaki, T., Kobayashi, T., Takagi, I.: Systematics of hydrolysis constants of tetravalent actinide ions. J. Nucl. Sci. Technol. **42**, 626 (2005).
4. Altmaier, M., Gaona, X., Fanghänel, Th.: Recent advances in aqueous actinide chemistry and thermodynamics. Chem. Rev. **113**, 901 (2013).
5. Grenthe, I., Fuger, J., Konings, R. J. M., Lemire, R. J., Müller, A. B., Nguyen-Trung, C., Wanner, H.: Chemical thermodynamics of uranium. In: H. Wanner, I. Forest (Eds.), Chemical Thermodynamics, Vol. 1, Elsevier, North-Holland, Amsterdam (1992).
6. Guillaumont, R., Fanghänel, Th., Fuger, J., Grenthe, I., Neck, V., Palmer, D., Rand, M.: Update on the chemical thermodynamics of uranium, neptunium, plutonium, americium and technetium. In: F. J. Mompean, M. Illemassene, C. Domenech-Orti, K. Ben Said (Eds.) Chemical thermodynamics, Vol. 5, Elsevier, North-Holland, Amsterdam (2003).
7. Rand, M., Fuger, J., Grenthe, I., Neck, V., Rai, D.: Chemical thermodynamics of thorium. In: F. J. Mompean, J. Perrone, M. Illemassene (Eds.) Chemical thermodynamics, Vol. 11, Elsevier, North-Holland, Amsterdam (2009).
8. Japan Nuclear Cycle Development Institute: 2nd progress report on research and development for the geological disposal of HLW in Japan, JNC Report TN1410 2000-001, JNC, Tokai, Japan (2000).
9. Office of Civilian Radioactive Waste Management: Yucca Mountain Science and Engineering Report Rev.1. DOE/RW-0539-1; OCRWM, North Las Vegas, NV (2002).
10. International Atomic Energy Agency: Geological disposal of radioactive waste: technological implications for retrievability; IAEA Nuclear Energy Series No. NWT-1.19, IAEA, Vienna (2009).
11. Katz, J. J., Seaborg, G. T., Morss, L. R.: The Chemistry of the Actinide Elements, Chapman and Hall, London (1986).
12. Hubert, S., Barthelet, K., Fourest, B., Lagarde, G., Dacheux, N., Baglan, N.: Influence of the precursor and the calcinations temperature on the dissolution of thorium dioxide. J. Nucl. Mater. **297**, 206 (2001).
13. Rai, D., Moore, D. A., Oakes, C. S., Yui, M.: Thermodynamic model for the solubility of thorium dioxide in the Na^+-Cl^--OH^--H_2O system at 23°C and 90°C. Radiochim. Acta **88**, 297 (2000).
14. Kobayashi, T., Sasaki, T., Takagi, I., Moriyama, H.: Effect of solid phase transformation on the solubility product of thorium hydrous oxide at 363 K. J. Nucl. Sci. Technol. **53**, 1787 (2016).
15. Baes, C. F., Meyer N. J., Roberts, C. E.: The hydrolysis of thorium(IV) at 0 and 95°. Inorg. Chem. **4**, 518 (1965).
16. Ekberg, C., Albinsson, Y., Comarmond, M. J., Brown, P. L.: Studies on the complexation behavior of thorium(IV). 1. Hydrolysis equilibria. J. Solution Chem. **29**, 63 (2000).
17. Teksöz, S., Acar, Ç., Ünak, P.: Hydrolytic behavior of Th^{4+}, UO_2^{2+}, and Ce^{3+} ions at various temperatures. Chem. Eng. Data **54**, 1183 (2009).
18. Kobayashi, T., Uemura, T., Sasaki, T., Takagi, I., Moriyama, H.: The solubilities and solubility products of zirconium hydroxide and oxide after aging at 278, 313, and 333 K. Radiochim. Acta **104**, 183 (2016).
19. Kobayashi, T., Bach, D., Altmaier, M., Sasaki, T., Moriyama, H.: Effect of temperature on the solubility and solid phase stability of zirconium hydroxide. Radiochim. Acta **101**, 645 (2013).
20. Moon, H.: Equilibrium ultrafiltration of hydrolyzed thorium(IV) solutions. Bull. Korean Chem. Soc. **10**, 270 (1989).

21. Östhols, E., Bruno, J., Grenthe, I.: On the influence of carbonate on mineral dissolution: III. The solubility of microcrystalline ThO_2 in CO_2-H_2O media. Geochim. Cosmochim. Acta **58**, 613 (1994).
22. Neck, V., Bouby, M., Altmaier, M., Rothe, J., Denecke, M. A., Kim, J. I.: Solubility of amorphous Th(IV) hydroxide - application of LIBD to determine the solubility product and EXAFS for aqueous speciation. Radiochim. Acta **90**, 485 (2002).
23. Neck, V., Altmaier, M., Müller, R., Bauer, A., Fanghänel, Th., Kim, J. I.: Solubility of crystalline thorium dioxide. Radiochim. Acta **91**, 253 (2003).
24. Kobayashi, T., Sasaki, T., Takagi, I., Moriyama, H.: Solubility of thorium(IV) in the presence of oxalic and malonic acids. J. Nucl. Sci. Technol. **46**, 1085 (2009).
25. Scherrer, P.: Bestimmung der Grösse und der inneren Struktur von Kolloidteilchen mittels Röntgenstrahlen [Determination of the size and internal structure of colloidal particles using X-rays]. Nachr. Ges. Wiss. Göttingen **26**, 98 (1918).
26. Sasaki, T., Takaoka, Y., Kobayashi, T., Fujii, T., Takagi, I., Moriyama, H.: Hydrolysis constants and complexation of Th(IV) with carboxylates. Radiochim. Acta **96**, 799 (2008).
27. Neck, V., Kim, J. I.: An electrostatic approach for the prediction of actinide complexation constants with inorganic ligands-application to carbonate complexes. Radiochim. Acta **88**, 815 (2000).
28. Stumm, W. and Morgan, J. J.: Aquatic Chemistry: Chemical Equilibria and Rates in Natural Waters, A Wiley-Interscience publication, New York (1996).
29. Bundschuh, T., Knopp, R., Müller, R., Kim, J. I., Neck, V., Fanghänel, Th.: Application of LIBD to the determination of the solubility product of thorium(IV)-colloids. Radiochim. Acta **88**, 625 (2000).
30. Schindler, P.: Heterogeneous equilibria involving oxides, hydroxides, carbonates, and hydroxide carbonates. Adv. Chem. Ser. **67**, 196 (1967).